

# Multi-objective optimization algorithms for finite element model updating

**E. Ntotsios and C. Papadimitriou**

University of Thessaly, Department of Mechanical and Industrial Engineering  
Volos 38334, Greece  
email: [costasp@mie.uth.gr](mailto:costasp@mie.uth.gr)

## Abstract

A multi-objective optimization method is presented for estimating the parameters of finite element structural models based on modal residuals. The method results in multiple Pareto optimal structural models that are consistent with the measured modal data and the modal residuals used to measure the discrepancies between the measured modal values and the modal values predicted by the finite element model. The relation between the multi-objective identification method and conventional single-objective weighted modal residuals methods for model updating is explored. Computationally efficient methods for estimating the gradient and Hessians of the objective functions with respect to the model parameters are proposed and shown to significantly reduce the computational effort for solving the single and multi-objective optimization problems. The proposed methods exploit Nelson's formulation for the sensitivity of the eigenproperties with respect to the parameters. Theoretical and computational developments are illustrated by updating finite element models of a multi-span reinforced concrete bridge using ambient vibration measurements. In particular, multi-objective identification results indicate that there is wide variety of Pareto optimal structural models that trade off the fit in various measured modal quantities.

## 1 Introduction

Structural model updating methods (e.g. [1]) have been proposed in the past to reconcile mathematical models, usually discretized finite element models, with experimental data. The estimate of the optimal model from a parameterized class of models is sensitive to uncertainties that are due to limitations of the mathematical models used to represent the behavior of the real structure, the presence of measurement and processing error in the data, the number and type of measured modal or response time history data used in the reconciling process, as well as the norms used to measure the fit between measured and model predicted characteristics. The optimal structural models resulting from such methods can be used for improving the model response and reliability predictions [2], structural health monitoring applications [3-6] and structural control [7].

Structural model parameter estimation problems based on measured data, such as modal characteristics (e.g. [3-6]) or response time history characteristics [8], are often formulated as weighted least-squares problems in which metrics, measuring the residuals between measured and model predicted characteristics, are build up into a single weighted residuals metric formed as a weighted average of the multiple individual metrics using weighting factors. Standard optimization techniques are then used to find the optimal values of the structural parameters that minimize the single weighted residuals metric representing an overall measure of fit between measured and model predicted characteristics. Due to model error and measurement noise, the results of the optimization are affected by the values assumed for the weighting factors. The model updating problem has also been formulated in a multi-objective context that allows the simultaneous minimization of the multiple metrics, eliminating the need for using arbitrary weighting factors for weighting the relative importance of each metric in the overall measure of fit. The multi-objective parameter estimation methodology provides multiple Pareto optimal structural models

consistent with the data and the residuals used in the sense that the fit each Pareto optimal model provides in a group of measured modal properties cannot be improved without deteriorating the fit in at least one other modal group.

In this work, the structural model updating problem using modal residuals is first formulated as a multi-objective optimization problem and then as a single-objective optimization with the objective formed as a weighted average of the multiple objectives using weighting factors. Theoretical and computational issues arising in multi-objective identification are addressed and the correspondence between the multi-objective identification and the weighted residuals identification is established. Emphasis is given in addressing issues associated with solving the resulting multi-objective and single-objective optimization problems. For this, efficient methods are proposed for estimating the gradients and the Hessians of the objective functions using the Nelson's method [9] for finding the sensitivities of the eigenproperties to model parameters. The proposed model updating methodologies are illustrated by updating a T-shaped R/C bridge structure, using ambient induced vibration measurements.

## 2 Model updating based on modal residuals

Let  $D = \{\hat{\omega}_r^{(k)}, \hat{\phi}_r^{(k)} \in R^{N_0}, r = 1, \dots, m, k = 1, \dots, N_D\}$  be the measured modal data from a structure, consisting of modal frequencies  $\hat{\omega}_r^{(k)}$  and modeshape components  $\hat{\phi}_r^{(k)}$  at  $N_0$  measured DOFs, where  $m$  is the number of observed modes and  $N_D$  is the number of modal data sets available. Consider a parameterized class of linear structural models used to model the dynamic behavior of the structure and let  $\underline{\theta} \in R^{N_\theta}$  be the set of free structural model parameters to be identified using the measured modal data. The objective in a modal-based structural identification methodology is to estimate the values of the parameter set  $\underline{\theta}$  so that the modal data  $\{\omega_r(\underline{\theta}), \phi_r(\underline{\theta}) \in R^{N_d}, r = 1, \dots, m\}$ , where  $N_d$  is the number of model degrees of freedom (DOF), predicted by the linear class of models best matches, in some sense, the experimentally obtained modal data in  $D$ . For this, let

$$\varepsilon_{\omega_r}(\underline{\theta}) = \frac{\omega_r^2(\underline{\theta}) - \hat{\omega}_r^2}{\hat{\omega}_r^2} \quad \text{and} \quad \varepsilon_{\phi_r}(\underline{\theta}) = \frac{\|\beta_r(\underline{\theta})L\phi_r(\underline{\theta}) - \hat{\phi}_r\|}{\|\hat{\phi}_r\|} \quad (1)$$

$r = 1, \dots, m$ , be the measures of fit or residuals between the measured modal data and the model predicted modal data for the  $r$ -th modal frequency and modeshape components, respectively, where  $\|\underline{z}\|^2 = \underline{z}^T \underline{z}$  is the usual Euclidian norm, and  $\beta_r(\underline{\theta}) = \hat{\phi}_r^T L\phi_r(\underline{\theta}) / \|L\phi_r(\underline{\theta})\|^2$  is a normalization constant that guaranties that the measured modeshape  $\hat{\phi}_r$  at the measured DOFs is closest to the model modeshape  $\beta_r(\underline{\theta})L\phi_r(\underline{\theta})$  predicted by the particular value of  $\underline{\theta}$ . The matrix  $L \in R^{N_0 \times N_d}$  is an observation matrix comprised of zeros and ones that maps the  $N_d$  model DOFs to the  $N_0$  observed DOFs.

In order to proceed with the model updating formulation, the measured modal properties are grouped into  $n$  groups. Each group contains one or more modal properties. The modal properties assigned in the  $i$ th group are identified by the set  $g_i(k)$ ,  $i = 1, \dots, n$  and  $k = 1, 2$ , with any element in the set  $g_i(k)$  is an integer from 1 to  $m$ . An element in the set  $g_i(k)$  with  $k = 1$  refer to the number of the measured modal frequency assigned in the group  $i$ , while the elements of the set  $g_i(k)$  with  $k = 2$  refer to the number of the measured modeshape assigned in the group  $i$ . For the  $i$ th group, a norm  $J_i(\underline{\theta})$  is introduced to measure the residuals of the difference between the measured values of the modal properties involved in the group and the corresponding modal values predicted from the model class for a particular value of the parameter set  $\underline{\theta}$ . The measure of fit in a modal group is the sum of the individual square errors in (1) for

the corresponding modal properties involved in the modal group. Specifically, the measure of fit is given by

$$J_i(\underline{\theta}) = \sum_{r \in g_i(1)} \varepsilon_{\omega_r}^2(\underline{\theta}) + \sum_{r \in g_i(2)} \varepsilon_{\phi_r}^2(\underline{\theta}) \quad (2)$$

The grouping of the modal properties  $\{\omega_r(\underline{\theta}), \phi_r(\underline{\theta}), r = 1, \dots, m\}$  into  $n$  groups and the selection of the measures of fit (residuals)  $J_1(\underline{\theta}), \dots, J_n(\underline{\theta})$  are usually based on user preference. The modal properties assigned to each group are selected by the user according to their type and the purpose of the analysis.

The aforementioned analysis accommodates general grouping schemes and objective functions. For demonstration purposes, a specific grouping scheme is next defined by grouping the modal properties into two groups as follows. The first group contains all modal frequencies, with the measure of fit  $J_1(\underline{\theta})$  selected to represent the difference between the measured and the model predicted frequencies for all modes, while the second group contains the modeshape components for all modes with the measure of fit  $J_2(\underline{\theta})$  selected to represent the difference between the measured and the model predicted modeshape components for all modes. Specifically, the two measures of fit are given by

$$J_1(\underline{\theta}) = \sum_{r=1}^m \varepsilon_{\omega_r}^2(\underline{\theta}) \quad \text{and} \quad J_2(\underline{\theta}) = \sum_{r=1}^m \varepsilon_{\phi_r}^2(\underline{\theta}) \quad (3)$$

The aforementioned grouping scheme is used in the application section for demonstrating the features of the proposed model updating methodologies.

## 2.1 Multi-objective identification

The problem of identifying the model parameter values that minimize the modal or response time history residuals can be formulated as a multi-objective optimization problem stated as follows [10]. Find the values of the structural parameter set  $\underline{\theta}$  that simultaneously minimizes the objectives

$$\underline{y} = \underline{J}(\underline{\theta}) = (J_1(\underline{\theta}), \dots, J_n(\underline{\theta})) \quad (4)$$

subject to inequality constraints  $\underline{c}(\underline{\theta}) \leq \underline{0}$  and parameter constraints  $\underline{\theta}_{low} \leq \underline{\theta} \leq \underline{\theta}_{upper}$ , where  $\underline{\theta} = (\theta_1, \dots, \theta_{N_\theta}) \in \Theta$  is the parameter vector,  $\Theta$  is the parameter space,  $\underline{y} = (y_1, \dots, y_n) \in Y$  is the objective vector,  $Y$  is the objective space,  $\underline{c}(\underline{\theta})$  is the vector function of constraints, and  $\underline{\theta}_{low}$  and  $\underline{\theta}_{upper}$  are respectively the lower and upper bounds of the parameter vector  $\underline{\theta}$ . For conflicting objectives  $J_1(\underline{\theta}), \dots, J_n(\underline{\theta})$ , there is no single optimal solution, but rather a set of alternative solutions, known as Pareto optimal solutions, that are optimal in the sense that no other solutions in the parameter space are superior to them when all objectives are considered. The set of objective vectors  $\underline{y} = \underline{J}(\underline{\theta})$  corresponding to the set of Pareto optimal solutions  $\underline{\theta}$  is called Pareto optimal front. The characteristics of the Pareto solutions are that the residuals cannot be improved in any group without deteriorating the residuals in at least one other group. The multiple Pareto optimal solutions are due to modeling and measurement errors.

Using multi-objective terminology, the Pareto optimal solutions are the non-dominating vectors in the parameter space  $\Theta$ , defined mathematically as follows. A vector  $\underline{\theta} \in \Theta$  is said to be non-dominated regarding the set  $\Theta$  if and only if there is no vector in  $\Theta$  which dominates  $\underline{\theta}$ . A vector  $\underline{\theta}$  is said to dominate a vector  $\underline{\theta}'$  if and only if

$$J_i(\underline{\theta}) \leq J_i(\underline{\theta}') \quad \forall i \in \{1, \dots, n\} \quad \text{and} \quad \exists j \in \{1, \dots, n\} : J_j(\underline{\theta}) < J_j(\underline{\theta}') \quad (5)$$

The set of objective vectors  $\underline{y} = \underline{J}(\underline{\theta})$  corresponding to the set of Pareto optimal solutions  $\underline{\theta}$  is called Pareto optimal front. The characteristics of the Pareto solutions are that the modal residuals cannot be improved in any modal group without deteriorating the modal residuals in at least one other modal group. Specifically, using the objective functions in (3), all optimal models that trade-off the overall fit in modal frequencies with the overall fit in the modeshapes are estimated.

The multiple Pareto optimal solutions are due to modelling and measurement errors. The level of modelling and measurement errors affect the size and the distance from the origin of the Pareto front in the objective space, as well as the variability of the Pareto optimal solutions in the parameter space. The variability of the Pareto optimal solutions also depends on the overall sensitivity of the objective functions or, equivalently, the sensitivity of the modal properties, to model parameter values  $\underline{\theta}$ . Such variabilities were demonstrated for the case of two-dimensional objective space and one-dimensional parameter space in the work by Christodoulou and Papadimitriou [11].

It should be noted that in the absence of modelling and measurement errors, there is an optimal value  $\hat{\underline{\theta}}$  of the parameter set  $\underline{\theta}$  for which the model based modal frequencies and modeshape components match exactly the corresponding measured modal properties. In this case, all objective functions  $J_1(\hat{\underline{\theta}}), \dots, J_n(\hat{\underline{\theta}})$  take the value of zero and, consequently, the Pareto front consists of a single point at the origin of the objective space. In particular, for identifiable problems [12-13], the solutions in the parameter space consist of one or more isolated points for the case of a single or multiple global optima, respectively. For non-identifiable problems [14-15], the Pareto optimal solutions form a lower dimensional manifold in the parameter space.

## 2.2 Weighted modal residuals identification

The parameter estimation problem is traditionally solved by minimizing the single objective

$$J(\underline{\theta}; \underline{w}) = \sum_{i=1}^n w_i J_i(\underline{\theta}) \quad (6)$$

formed from the multiple objectives  $J_i(\underline{\theta})$  using the weighting factors  $w_i \geq 0$ ,  $i = 1, \dots, n$ , with  $\sum_{i=1}^n w_i = 1$ . The objective function  $J(\underline{\theta}; \underline{w})$  represents an overall measure of fit between the measured and the model predicted characteristics. The relative importance of the residual errors in the selection of the optimal model is reflected in the choice of the weights. The results of the identification depend on the weight values used. Conventional weighted least squares methods assume equal weight values,  $w_1 = \dots = w_n = 1/n$ . This conventional method is referred herein as the equally weighted modal residuals method.

## 2.3 Comparison between multi-objective and weighted modal residuals identification

Formulating the parameter identification problem as a multi-objective minimization problem, the need for using arbitrary weighting factors for weighting the relative importance of the residuals  $J_i(\underline{\theta})$  of a modal group to an overall weighted residuals metric is eliminated. An advantage of the multi-objective identification methodology is that all admissible solutions in the parameter space are obtained.

It can be readily shown that the optimal solution to the problem (6) is one of the Pareto optimal solutions. For this, let  $\hat{\underline{\theta}}$  be the global optimal solution that minimizes the objective function  $J(\underline{\theta}; \underline{w})$  in (6) for given  $\underline{w}$ . Then this solution is also a Pareto optimal solution since otherwise there would exist another

solution, say  $\underline{\hat{\theta}}'$ , for which equation (5) will be satisfied for  $\underline{\theta} = \underline{\hat{\theta}}'$  and  $\underline{\theta}' = \underline{\hat{\theta}}$ , that is,  $J_i(\underline{\hat{\theta}}') \leq J_i(\underline{\hat{\theta}}) \quad \forall i \in \{1, \dots, n\}$  and  $\exists j \in \{1, \dots, n\} : J_j(\underline{\hat{\theta}}') < J_j(\underline{\hat{\theta}})$ . As a result of this and the fact that  $w_i \geq 0$ , it is readily derived using the form of  $J(\underline{\theta}; \underline{w})$  in (6) that  $J(\underline{\hat{\theta}}'; \underline{w}) < J(\underline{\hat{\theta}}; \underline{w})$ . The last inequality implies that  $\underline{\hat{\theta}}'$ , instead of  $\underline{\hat{\theta}}$ , is the global solution optimizing  $J(\underline{\theta}; \underline{w})$ , which is a contradiction.

Thus, solving a series of single objective optimization problems of the type (6) and varying the values of the weights  $w_i$  from 0 to 1, excluding the case for which the values of all weights are simultaneously equal to zero, Pareto optimal solutions are alternatively obtained. These solutions for given  $\underline{w}$  are denoted by  $\underline{\hat{\theta}}(\underline{w})$ . It should be noted, however, that there may exist Pareto optimal solutions that do not correspond to solutions of the single-objective weighted modal residuals problem [16].

The single objective is computationally attractive since conventional minimization algorithms can be applied to solve the problem. However, a severe drawback of generating Pareto optimal solutions by solving the series of weighted single-objective optimization problems by uniformly varying the values of the weights is that this procedure often results in cluster of points in parts of the Pareto front that fail to provide an adequate representation of the entire Pareto shape. Thus, alternative algorithms dealing directly with the multi-objective optimization problem and generating uniformly spread points along the entire Pareto front should be preferred. Special algorithms are available for solving the multi-objective optimization problem. Computational algorithms and related issues for solving the single-objective and the multi-objective optimization problems are discussed in Section 3.

### 3 Computational Issues Related to Model Updating Formulations

The proposed single and multi-objective identification problems are solved using available single- and multi-objective optimization algorithms. These algorithms are briefly reviewed and various implementation issues are addressed, including estimation of global optima from multiple local/global ones, as well as convergence problems.

#### 3.1 Single-Objective Identification

The optimization of  $J(\underline{\theta}; \underline{w})$  in (6) with respect to  $\underline{\theta}$  for given  $\underline{w}$  can readily be carried out numerically using any available algorithm for optimizing a nonlinear function of several variables. These single objective optimization problems may involve multiple local/global optima. Conventional gradient-based local optimization algorithms lack reliability in dealing with the estimation of multiple local/global optima observed in structural identification problems [10,17], since convergence to the global optimum is not guaranteed. Evolution strategies (ES) [18] are more appropriate and effective to use in such cases. ES are random search algorithms that explore better the parameter space for detecting the neighborhood of the global optimum, avoiding premature convergence to a local optimum. A disadvantage of ES is their slow convergence at the neighborhood of an optimum since they do not exploit the gradient information. A hybrid optimization algorithm should be used that exploits the advantages of ES and gradient-based methods. Specifically, an evolution strategy is used to explore the parameter space and detect the neighborhood of the global optimum. Then the method switches to a gradient-based algorithm starting with the best estimate obtained from the evolution strategy and using gradient information to accelerate convergence to the global optimum.

### 3.2 Multi-Objective Identification

The set of Pareto optimal solutions can be obtained using available multi-objective optimization algorithms. Among them, the evolutionary algorithms, such as the strength Pareto evolutionary algorithm [19], are well-suited to solve the multi-objective optimization problem. The strength Pareto evolutionary algorithm, although it does not require gradient information, it has the disadvantage of slow convergence for objective vectors close to the Pareto front [10] and also it does not generate an evenly spread Pareto front, especially for large differences in objective functions.

Another very efficient algorithm for solving the multi-objective optimization problem is the Normal-Boundary Intersection (NBI) method [20] which produce an evenly spread of points along the Pareto front, even for problems for which the relative scaling of the objectives are vastly different. For completeness and for the purpose of demonstrating the implementation issues arising in multi-objective structural model updating, the idea of the NBI method is briefly illustrated geometrically with the aid of the two-dimensional Pareto front shown in Figure 1. For this, let  $\hat{\theta}^{(i)}$ ,  $i = 1, \dots, n$ , be the global optimal values of the parameter set that minimize the individual objectives  $J_i(\theta)$ ,  $i = 1, \dots, n$ , respectively. The Pareto points  $\hat{J}^{(i)} = J(\hat{\theta}^{(i)})$ , shown in Figure 1, determine the location of the boundaries of the Pareto front in the objective space. These edge points of the Pareto front are estimated using the single-objective optimization algorithms outlined in Section 3.1. The utopia point  $\hat{J} = [\hat{J}_1, \dots, \hat{J}_n]^T$ , shown in Figure 1, is introduced as the point in the objective space with coordinates the individual minima  $\hat{J}_i = J_i(\hat{\theta}^{(i)})$  of the objectives. Let  $\Phi$  be the  $n \times n$  matrix with the  $i$ -th column equal to the vector  $\hat{J}^{(i)}$ . The set of points in the objective space that are convex combinations of  $\hat{J}^{(i)} - \hat{J}$ , obtained by the points  $\{\Phi\beta : \beta \in R^n, \sum_{i=1}^n \beta_i = 1, \beta_i \geq 0\}$ , is referred to as the Convex Hull of Individual Minima (CHIM). These points are all points along the line segment AB in Figure 1. The Pareto points consist of points on the intersection of the boundary  $\partial Y$  of the objective space  $Y$  and the normal initiating from any point in the CHIM and pointing towards the origin of the objective space.

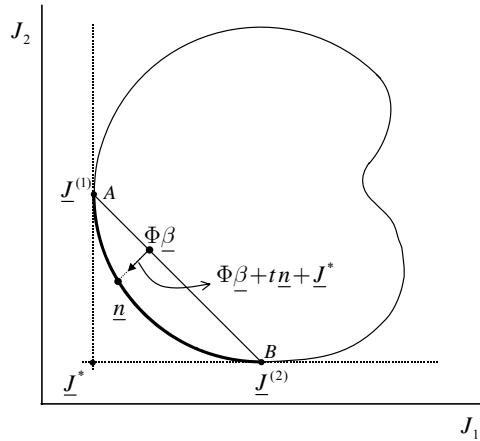


**Figure 1. Geometric illustration of NBI Method in 2-dimensional objective space**

A point along the Pareto front can be found by solving a single-objective optimization problem. Given the coordinates  $\beta$ ,  $\Phi\beta$  represents a point on the CHIM and  $\Phi\beta + t\underline{n}$ , where  $t \in R$  and  $\underline{n}$  the normal to the CHIM, represents the set of points on the normal to the CHIM at the point  $\Phi\beta$ . The point of intersection

of the normal and the boundary  $\partial Y$ , closest to the origin, is the global solution of the commonly referred as NBI $_{\underline{\beta}}$  optimization problem [20]:

$$\max_{\underline{\theta}, t} t \quad (7)$$

subject to the constraints

$$\Phi \underline{\beta} + t \underline{n} = \underline{J}(\underline{\theta}) - \underline{J}^* \quad (8)$$

Any constraints from the original multi-objective optimization problem (4) can also be considered by adding them as constraints in the NBI $_{\underline{\beta}}$  optimization problem. By solving the optimization problems NBI $_{\underline{\beta}}$  for various  $\underline{\beta}$  values in the set  $\{\underline{\beta} \in \mathbb{R}^n : \sum_{i=1}^n \beta_i = 1, \beta_i \geq 0\}$ , a pointwise representation of the Pareto front is efficiently constructed. The values of the parameters  $\underline{\beta}$  are selected so that an evenly spread points along the CHIM are obtained, resulting to an evenly spread points along the Pareto front, independently of the scales of the objective functions. For the two-dimensional objective space, this is achieved by selecting the values of the component  $\beta_2$  of  $\underline{\beta} = (\beta_1, \beta_2)$  to be uniformly spaced in the interval  $[0,1]$  with spacing length  $\delta = 1/(N-1)$ , where  $N$  is the number of points along the CHIM including the edge points. The first component  $\beta_1$  is selected to satisfy  $\beta_1 + \beta_2 = 1$ . More details about the method, the selection of  $\underline{\beta}$  values for more than two objectives, advantages and drawbacks, can be found in the original paper by Das and Dennis [20].

It is also of interest to compare the computational time involved for estimating the Pareto optimal solutions with the computational time required in conventional weighted residuals methods for estimating a single solution. This estimate can be made by noting that each Pareto optimal solutions is obtained by solving a single-objective optimization problem NBI $_{\underline{\beta}}$ . Thus, this computational time is of the order of the number of points used to represent the Pareto front multiplied by the computational time required to solve a single-objective NBI $_{\underline{\beta}}$  problem for computing each point on the front. However, for the NBI method, convergence can be greatly accelerated by using a good starting value for the NBI $_{\underline{\beta}}$  optimization problem close to the optimal value. This is achieved by selecting the Pareto optimal solution obtained from the current NBI $_{\underline{\beta}}$  problem to be used as starting value for solving the next NBI $_{\underline{\beta}}$  problem.

### 3.3 Formulation for gradients of objectives

In order to guarantee the convergence of the gradient-based optimization methods for structural models involving a large number of DOFs with several contributing modes, the gradients of the objective functions with respect to the parameter set  $\underline{\theta}$  has to be estimated accurately. It has been observed that numerical algorithms such as finite difference methods for gradient evaluation does not guarantee convergence due to the fact that the errors in the numerical estimation may provide the wrong directions in the search space and convergence to the local/global minimum is not achieved, especially for intermediate parameter values in the vicinity of a local/global optimum. Thus, the gradients of the objective functions should be provided analytically. Moreover, gradient computations with respect to the parameter set using the finite difference method requires the solution of as many eigenvalue problems as the number of parameters.

The gradients of the modal frequencies and modeshapes, required in the estimation of the gradient of  $J(\underline{\theta}; \underline{w})$  in (6) or the gradients of the objectives  $J_i(\underline{\theta})$  in (4) are computed by expressing them exactly in terms of the modal frequencies, modeshapes and the gradients of the structural mass and stiffness matrices with respect to  $\underline{\theta}$  using Nelson's method [9]. Special attention is given to the computation of the gradients

and the Hessians of the objective functions for the point of view of the reduction of the computational time required. Analytical expressions for the gradient of the modal frequencies and modeshapes are used to overcome the convergence problems. In particular, Nelson's method [9] is used for computing analytically the first derivatives of the eigenvalues and the eigenvectors. The advantage of the Nelson's method compared to other methods is that the gradient of eigenvalue and the eigenvector of one mode are computed from the eigenvalue and the eigenvector of the same mode and there is no need to know the eigenvalues and the eigenvectors from other modes. For each parameter in the set  $\underline{\theta}$  this computation is performed by solving a linear system of the same size as the original system mass and stiffness matrices. Nelson's method is also extended in Section 3.4 to compute the second derivatives of the eigenvalues and the eigenvectors.

The computation of the gradients and the Hessian of the objective functions is shown to involve the solution of a single linear system, instead of  $N_\theta$  linear systems required in usual computations of the gradient and  $N_\theta(N_\theta + 1)$  linear systems required in the computation of the Hessian. This reduces considerably the computational time, especially as the number of parameters in the set  $\underline{\theta}$  increase. The expressions for the first derivatives of the objective functions are next presented.

Summarizing, Nelson's method [9] specialized for symmetric mass and stiffness matrices computes the derivatives of the  $r$ -th eigenvalue and eigenvector with respect to a parameter  $\theta_j$  in the parameter set  $\underline{\theta}$  from the following formulas

$$\frac{\partial \omega_r^2}{\partial \theta_j} = \underline{\phi}_r^T (K_j - \omega_r^2 M_j) \underline{\phi}_r \quad (9)$$

and

$$\frac{\partial \underline{\phi}_r}{\partial \theta_j} = (I - \underline{\phi}_r \underline{\phi}_r^T M) A_r^{*-1} \underline{F}_r^* - \frac{1}{2} \underline{\phi}_r \underline{\phi}_r^T M_j \underline{\phi}_r \quad (10)$$

where

$$A_r = K - \omega_r^2 M \quad (11)$$

$$\underline{F}_{r,j} = -\frac{\partial A_r}{\partial \theta_j} \underline{\phi}_r = -(I - M \underline{\phi}_r \underline{\phi}_r^T) (K_j - \omega_r^2 M_j) \underline{\phi}_r \quad (12)$$

$$M_j \equiv M_j(\underline{\theta}) = \frac{\partial M(\underline{\theta})}{\partial \theta_j}, \quad K_j \equiv K_j(\underline{\theta}) = \frac{\partial K(\underline{\theta})}{\partial \theta_j} \quad (13)$$

For notational convenience, the dependence of several variables on the parameter set  $\underline{\theta}$  has been dropped. For an  $n \times n$  matrix  $A_r$  referring to the formulation for the  $r$ -th mode,  $A_r^*$  is used to denote the modified matrix derived from the matrix  $A_r$  by replacing the elements of the  $k$ -th column and the  $k$ -th row by zeroes and the  $(k, k)$  element of  $A_r$  by one, where  $k$  denotes the element of the modeshape vector  $\underline{\phi}_r$  with the highest absolute value. Also, the  $n$  vector  $\underline{b}_r^*$  is used to denote the modified vector derived from  $\underline{b}_r$  replacing the  $k$ -th element of the vector  $\underline{b}_r$  by zero. More details can be found in the work by Nelson [9].

The gradient of the square error  $\varepsilon_{\omega_r}^2(\underline{\theta})$  is given by

$$\frac{\partial \varepsilon_{\omega_r}^2(\underline{\theta})}{\partial \theta_j} = \frac{\partial \varepsilon_{\omega_r}^2(\underline{\theta})}{\partial \omega_r^2} \frac{\partial \omega_r^2}{\partial \theta_j} = \left[ \frac{\partial \varepsilon_{\omega_r}^2(\underline{\theta})}{\partial \omega_r^2} \underline{\phi}_r^T \right] (K_j - \omega_r^2 M_j) \underline{\phi}_r \quad (14)$$



and the gradient of the square error  $\varepsilon_{\underline{\phi}_r}^2(\underline{\theta})$  is given by

$$\frac{\partial \varepsilon_{\underline{\phi}_r}^2(\underline{\theta})}{\partial \theta_j} = [\nabla_{\underline{\phi}_r}^T \varepsilon_{\underline{\phi}_r}^2(\underline{\theta})] \frac{\partial \underline{\phi}_r}{\partial \theta_j} = [\nabla_{\underline{\phi}_r}^T \varepsilon_{\underline{\phi}_r}^2(\underline{\theta})] L \frac{\partial \underline{\phi}_r}{\partial \theta_j} \quad (15)$$

Substituting (10) into (15), the gradient of the square error  $\varepsilon_{\underline{\phi}_r}^2(\underline{\theta})$  is simplified to

$$\frac{\partial \varepsilon_{\underline{\phi}_r}^2(\underline{\theta})}{\partial \theta_j} = \underline{x}_r^{*T} \underline{F}_{r,j} - \frac{1}{2} \underline{z}_r^T \underline{M}_j \underline{\phi}_r \quad (16)$$

where  $\underline{F}_{r,j}$  is given in (12),

$$\underline{z}_r^T = [\nabla_{\underline{\phi}_r}^T \varepsilon_{\underline{\phi}_r}^2(\underline{\theta})] L \underline{\phi}_r \underline{\phi}_r^T \quad (17)$$

and  $\underline{x}_r$  is given by the solution of the linear system of equations

$$\underline{A}_r^* \underline{X}_r = \underline{D}_r \quad (18)$$

with  $\underline{D}_r = (I - \underline{M} \underline{\phi}_r \underline{\phi}_r^T) L^T \nabla_{\underline{\phi}_r} \varepsilon_{\underline{\phi}_r}^2(\underline{\theta})$  and  $\underline{X}_r$  replaced by  $\underline{x}_r$ . The system of equations (18) can be viewed as the adjoint system for the model updating optimization problem based on modal residuals.

It should be noted that for the specific objective functions  $\varepsilon_{\omega_r}^2(\underline{\theta})$  and  $\varepsilon_{\underline{\phi}_r}^2(\underline{\theta})$  given by (1), the aforementioned expressions for the gradients of the objective functions simplify further. Specifically, using (1) and noting that  $\varepsilon_{\underline{\phi}_r}^T(\underline{\theta}) L \underline{\phi}_r = \varepsilon_{\underline{\phi}_r}^T(\underline{\theta}) \underline{\phi}_r = 0$ , one readily obtains that

$$\frac{\partial \varepsilon_{\omega_r}^2(\underline{\theta})}{\partial \omega_r^2} = \frac{2 \varepsilon_{\omega_r}(\underline{\theta})}{\hat{\omega}_r^2} \quad (19)$$

$$\nabla_{\underline{\phi}_r} \varepsilon_{\underline{\phi}_r}^2(\underline{\theta}) = 2 \underline{e}_{\underline{\phi}_r}(\underline{\theta}) \beta_r \quad (20)$$

where

$$\underline{e}_{\underline{\phi}_r} = \frac{\beta_r L \underline{\phi}_r^T - \hat{\underline{\phi}}_r^T}{\|\hat{\underline{\phi}}_r\|^2} \quad (21)$$

$\underline{z}_r^T = \underline{0}^T$  and  $\underline{D}_r$  is given by the equation

$$\underline{D}_r = L^T 2 \beta_r \underline{e}_{\underline{\phi}_r}(\underline{\theta}) \quad (22)$$

The computation of the derivatives of the square errors for the modal properties of the  $r$ -th mode with respect to the parameters in  $\underline{\theta}$  requires only one solution of the linear system (18), independent of the number of parameters in  $\underline{\theta}$ . For a large number of parameters in the set  $\underline{\theta}$  the above formulation for the gradients of the mean errors in modal frequencies and in the modeshape components in (1) are computationally very efficient and informative. The dependence on  $\theta_j$  comes through the term  $K_j - \omega_r^2 M_j$  and the term  $M_j$ . For the case where the mass matrix is independent of  $\underline{\theta}$ ,  $M_j = 0$  and the formulation is further simplified.

It should be noted that for the special case of linear dependence between the global mass and stiffness matrices on the parameters in the set  $\underline{\theta}$ , that is,  $M(\underline{\theta}) = M_0 + \sum_{j=1}^{N_\theta} M_j \theta_j$  and

$K(\underline{\theta}) = K_0 + \sum_{j=1}^{N_\theta} K_j \theta_j$ , the gradients of  $M(\underline{\theta})$  and  $K(\underline{\theta})$  are easily computed from the constant matrices  $M_0$ ,  $K_0$ ,  $M_j$  and  $K_j$ ,  $j=1, \dots, N_\theta$ . In order to save computational time, these constant matrices are computed and assembled once and, therefore, there is no need this computation to be repeated during the iterations involved in optimization algorithms. For the general case of nonlinear dependence between the global mass and stiffness matrices on the parameters in the set  $\underline{\theta}$ , the matrices  $M_j$  and  $K_j$  involved in the formulation (see (13)) can be obtained numerically at the element level and assembled to form the global matrices.

### 3.4 Formulation for Hessian of objectives

A similar analysis to that followed in Nelson's method [9] for computing the first derivative can also be followed for computing the second derivatives of the eigenvalues and the eigenvectors, resulting in the following expressions for the second derivatives

$$\frac{\partial^2 \omega_r^2}{\partial \theta_i \partial \theta_j} = \underline{\phi}_r^T \underline{g}_{r,ij} \quad (23)$$

and

$$\frac{\partial^2 \underline{\phi}_r}{\partial \theta_i \partial \theta_j} = (I - \underline{\phi}_r \underline{\phi}_r^T M) A_r^{*-1} \underline{G}_r - \underline{\phi}_r d_{r,ij} \quad (24)$$

where

$$\underline{G}_r = -(I - M \underline{\phi}_r \underline{\phi}_r^T) \underline{g}_r \quad (25)$$

$$\underline{g}_{r,ij} = \frac{\partial A_r}{\partial \theta_i} \frac{\partial \underline{\phi}_r}{\partial \theta_j} + \frac{\partial A_r}{\partial \theta_j} \frac{\partial \underline{\phi}_r}{\partial \theta_i} + \left[ \frac{\partial^2 K}{\partial \theta_i \partial \theta_j} - \lambda_r \frac{\partial^2 M}{\partial \theta_i \partial \theta_j} - \frac{\partial \lambda_r}{\partial \theta_i} \frac{\partial M}{\partial \theta_j} - \frac{\partial \lambda_r}{\partial \theta_j} \frac{\partial M}{\partial \theta_i} \right] \underline{\phi}_r \quad (26)$$

and

$$d_{r,ij} = \underline{\phi}_r^T \left[ \frac{\partial M}{\partial \theta_i} \frac{\partial \underline{\phi}_r}{\partial \theta_j} + \frac{\partial M}{\partial \theta_j} \frac{\partial \underline{\phi}_r}{\partial \theta_i} + \frac{1}{2} \frac{\partial^2 M}{\partial \theta_i \partial \theta_j} \underline{\phi}_r \right] + \frac{\partial \underline{\phi}_r^T}{\partial \theta_i} M \frac{\partial \underline{\phi}_r}{\partial \theta_j} \quad (27)$$

The Hessian of the objective functions  $\varepsilon_{\omega_r}^2(\underline{\theta})$  and  $\varepsilon_{\underline{\phi}_r}^2(\underline{\theta})$  can be readily computed from the second derivatives of the eigenvalues and the eigenvectors, respectively. Specifically, the  $(i, j)$  element of the Hessian of  $\varepsilon_{\omega_r}^2(\underline{\theta})$  is obtained by differentiating (14) with respect to  $\theta_i$ , resulting in

$$\begin{aligned} \frac{\partial^2 \varepsilon_{\omega_r}^2(\underline{\theta})}{\partial \theta_i \partial \theta_j} &= \frac{\partial^2 \varepsilon_{\omega_r}^2(\underline{\theta})}{\partial (\omega_r^2)^2} \frac{\partial \omega_r^2}{\partial \theta_i} \frac{\partial \omega_r^2}{\partial \theta_j} + \frac{\partial \varepsilon_{\omega_r}^2(\underline{\theta})}{\partial \omega_r^2} \frac{\partial^2 \omega_r^2}{\partial \theta_i \partial \theta_j} \\ &= \frac{\partial^2 \varepsilon_{\omega_r}^2(\underline{\theta})}{(\partial \omega_r^2)^2} [\underline{\phi}_r^T (K_i - \omega_r^2 M_i) \underline{\phi}_r] [\underline{\phi}_r^T (K_j - \omega_r^2 M_j) \underline{\phi}_r] + \frac{\partial \varepsilon_{\omega_r}^2(\underline{\theta})}{\partial \omega_r^2} \underline{\phi}_r^T \underline{g}_r \end{aligned} \quad (28)$$

The  $(i, j)$  element of the Hessian of  $\varepsilon_{\underline{\phi}_r}^2(\underline{\theta})$  is obtained by differentiating (15) with respect to  $\theta_i$ , resulting in

$$\frac{\partial^2 \varepsilon_{\underline{\phi}_r}^2(\underline{\theta})}{\partial \theta_i \partial \theta_j} = \frac{\partial \underline{\phi}_r^T}{\partial \theta_i} [\nabla_{\underline{\phi}_r} \nabla_{\underline{\phi}_r}^T \varepsilon_{\underline{\phi}_r}^2(\underline{\theta})] \frac{\partial \underline{\phi}_r}{\partial \theta_j} + [\nabla_{\underline{\phi}_r}^T \varepsilon_{\underline{\phi}_r}^2(\underline{\theta})] \frac{\partial^2 \underline{\phi}_r}{\partial \theta_i \partial \theta_j} \quad (29)$$

Substituting (24) into (29) and using (18), the Hessian can be finally simplified to

$$\frac{\partial^2 \varepsilon_{\phi_r}^2(\underline{\theta})}{\partial \theta_i \partial \theta_j} = \frac{\partial \underline{\phi}_r^T}{\partial \theta_i} L^T [\nabla_{\underline{\phi}_r} \nabla_{\underline{\phi}_r} \varepsilon_{\phi_r}^2(\underline{\theta})]^T L \frac{\partial \underline{\phi}_r}{\partial \theta_j} - 2 \underline{x}_r^{*T} (I - M \underline{\phi}_r \underline{\phi}_r^T) \underline{g}_r - 2 [\nabla_{\underline{\phi}_r}^T \varepsilon_{\phi_r}^2(\underline{\theta})] L \underline{\phi}_r d_{r,ij} \quad (30)$$

It should be noted that for the specific objective functions  $\varepsilon_{\omega_r}^2(\underline{\theta})$  and  $\varepsilon_{\phi_r}^2(\underline{\theta})$  given by (1), the aforementioned expressions for the Hessian of the objective functions simplify further. Specifically, using (1) and noting that  $\varepsilon_{\phi_r}^T(\underline{\theta}) L \underline{\phi}_r = \varepsilon_{\phi_r}^T(\underline{\theta}) \underline{\phi}_r = 0$ , one readily obtains that

$$\frac{\partial^2 \varepsilon_{\omega_r}^2(\underline{\theta})}{\partial (\omega_r^2)^2} = \frac{2}{\hat{\omega}_r^4} \quad (31)$$

$$\nabla_{\underline{\phi}_r} \nabla_{\underline{\phi}_r}^T \varepsilon_{\phi_r}^2(\underline{\theta}) = \frac{-2}{\|\hat{\underline{\phi}}_r\|^2 \|\underline{\phi}_r\|^2} \left[ (2\beta_r \underline{\phi}_r - \hat{\underline{\phi}}_r)(2\beta_r \underline{\phi}_r - \hat{\underline{\phi}}_r)^T - \beta_r^2 \|\underline{\phi}_r\|^2 I \right] \quad (32)$$

and  $\frac{\partial^2 \varepsilon_{\phi_r}^2(\underline{\theta})}{\partial \theta_i \partial \theta_j}$  in (30) simplifies to

$$\frac{\partial^2 \varepsilon_{\phi_r}^2(\underline{\theta})}{\partial \theta_i \partial \theta_j} = -\frac{2}{\|\hat{\underline{\phi}}\|^2 \|\underline{L}\underline{\phi}_r\|^2} \left( \underline{z}_r^{*T} \underline{F}_{r,i} \right) \left( \underline{z}_r^{*T} \underline{F}_{r,j} \right) - \beta_r^2 \|\underline{L}\underline{\phi}_r\|^2 \underline{F}_{r,j}^{*T} \underline{X}_r \underline{X}_r^T \underline{F}_{r,i}^* - 2 \underline{x}_r^{*T} (I - M \underline{\phi}_r \underline{\phi}_r^T) \underline{g}_r \quad (33)$$

where  $\underline{z}_r$  is given by the solution of the linear system (18) with  $D_r = (I - M^T \underline{\phi}_r \underline{\phi}_r^T) L^T (2\beta_r \underline{L}\underline{\phi}_r - \hat{\underline{\phi}}_r)$  and  $\underline{X}_r$  is given by (18) with  $D_r = (I - M^T \underline{\phi}_r \underline{\phi}_r^T) L^T$ .

It should be noted that only the last term in (28) and the last term in (33) depend explicitly on the derivatives  $\partial \underline{\phi}_r / \partial \theta_i$ . Numerical results suggest that the Hessian of  $\varepsilon_{\omega_r}^2(\underline{\theta})$  and  $\varepsilon_{\phi_r}^2(\underline{\theta})$  can be adequately approximated in the form (28) and (33), ignoring the contribution from the last terms in (28) and (33). Thus the Hessian of  $\varepsilon_{\omega_r}^2(\underline{\theta})$  and  $\varepsilon_{\phi_r}^2(\underline{\theta})$  can be computed from the solution of the system (18), estimates of the eigenvalues and eigenvectors of the mode  $r$ , and the sensitivities  $K_j$  and  $M_j$  of the global stiffness and mass matrices with respect to the parameters  $\underline{\theta}$ .

Summarizing, it should be noted that the computation of the first and second derivatives of the square errors for the modal properties of the  $r$ -th mode with respect to the parameters in  $\underline{\theta}$  requires only the solutions of the linear system (18), independent of the number of parameters in  $\underline{\theta}$ . For a large number of parameters in the set  $\underline{\theta}$ , the above formulation for the gradients and Hessian of the mean errors in modal frequencies and in the modeshape components in (1) are computationally very efficient and informative.

## 4 Application

The proposed framework has been applied to a T-shaped R/C bridge (Figure 2a) of Egnatia Odos motorway which crosses Northern Greece in the east-west direction. The is located at Polymylos and has been instrumented with special array of 24 accelerometers. The response to ambient excitation caused by traffic and wind has been systematically monitored. The modal identification using these ambient vibrations resulted in the reliable estimation of the first eight modes. To implement the model updating techniques, an appropriate parametric finite element model of the bridge is considered using three-dimensional two-node beam-type finite elements to model the deck, the piers and the bearings. This model is shown in Figure 2b and has 1038 degrees of freedom. The entire simulation is performed within the

COMSOL Multiphysics [21] modeling environment. A three parameter model class is employed in order to demonstrate the applicability of the proposed methodologies, and point out issues associated with the multi-objective identification. The first parameter  $\theta_1$  accounts for the stiffness of the elastomeric bearings at the abutments, the second parameter  $\theta_2$  accounts for the stiffness of the deck, while the third parameter  $\theta_3$  accounts for the stiffness of the piers. The nominal finite element model corresponds to values of  $\theta_1 = \theta_2 = \theta_3 = 1$ . The parameterized finite element model class is updated using the three modal frequencies and modeshapes obtained from operational modal analysis and the two modal groups with modal residuals given by (3).

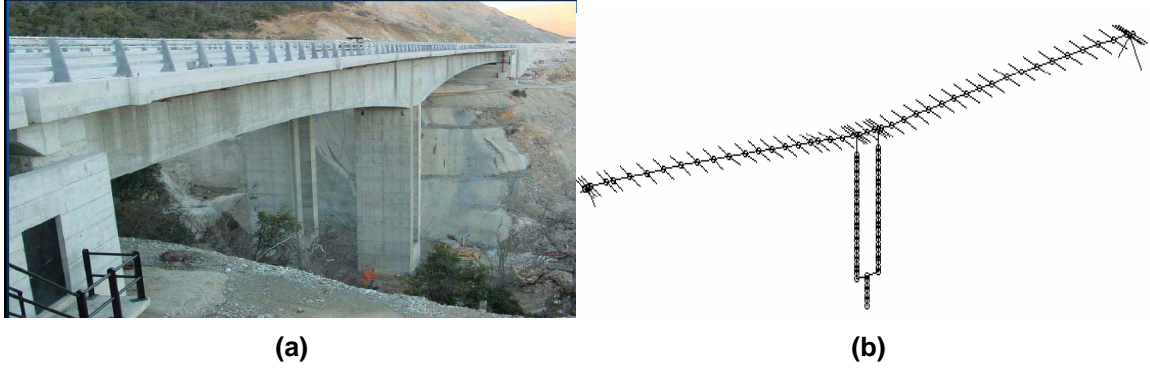


**Figure 2: (a) View of the Polymylos bridge, (b) Finite element model.**

The results from the multi-objective identification methodology are shown in Figure 3. For each model class and associated structural configuration, the Pareto front, giving the Pareto solutions in the two-dimensional objective space, is shown in Figure 3a. The non-zero size of the Pareto front and the non-zero distance of the Pareto front from the origin are due to modeling and measurement errors. Specifically, the distance of the Pareto points along the Pareto front from the origin is an indication of the size of the overall measurement and modeling error. The size of the Pareto front depends on the size of the model error and the sensitivity of the modal properties to the parameter values  $\underline{\theta}$  [16]. Figures 3b-d show the corresponding Pareto optimal solutions in the three-dimensional parameter space. Specifically, these figures show the projection of the Pareto solutions in the two-dimensional parameter spaces  $(\theta_1, \theta_2)$ ,  $(\theta_1, \theta_3)$  and  $(\theta_2, \theta_3)$ .

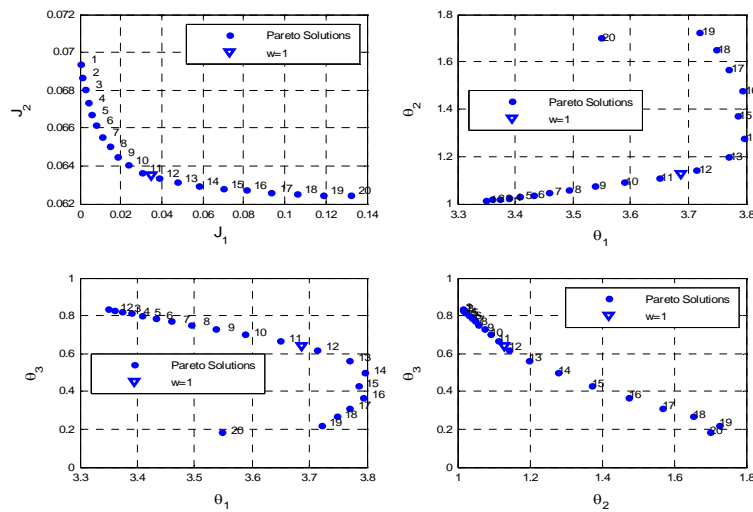


**Figure 3: Pareto front and Pareto optimal solutions in the (a) objective space and (b-d) parameter space**

It is observed that a wide variety of Pareto optimal solutions are obtained for different structural configurations that are consistent with the measured data and the objective functions used. The Pareto optimal solutions are concentrated along a one-dimensional manifold in the three-dimensional parameter space. Comparing the Pareto optimal solutions, it can be said that there is no Pareto solution that improves the fit in both modal groups simultaneously. Thus, all Pareto solutions correspond to acceptable compromise structural models trading-off the fit in the modal frequencies involved in the first modal group with the fit in the modeshape components involved in the second modal groups.

The effectiveness of the analytic expressions for the gradients and the Hessian of the objective functions (3) involved on the solution of the model updating problem has been investigated by updating the finite element model of the Polymylos bridge using simulated modal data. Specifically, three parameterized model classes were updated using 12 simulated modes and applying the Newton Trust-region non-linear optimization method [23] and the BFGS quasi-Newton method [25]. The parameterized model classes that were updated included a limited number of 3, 5 and 7 parameters. For the 3-parameter model class the first parameter accounts for the stiffness of the elastomeric bearings at the abutments, the second parameter accounts for the stiffness of the deck, while the third parameter accounts for the stiffness of the piers. For the 5-parameter model class the extra two parameters were introduced to model the stiffness that was assumed independent for the left and right bearings of the bridge and the two columns at the central pier. For the 7-parameter model class the extra two parameters were introduced to model the stiffness of the bearings that was assumed independent along the longitudinal and transverse direction of the bridge.

The effectiveness of the proposed optimization schemes is investigated comparing the convergence and the computational time for each method and for each parameterized model class. A comparison between the optimization methods concerning convergence (number of iterations) and computational time is presented in Table 1. The values in Table 1 referred to the BFGS medium-scale optimization algorithm show that this optimization scheme is superior for the solution of the specific problem for all model classes. The number of iterations required for the Newton Trust-region large-scale optimization method using the analytic expressions of the Hessian matrix is of the same order of magnitude as the number of iterations required for the BFGS method. The computational time for the Newton Trust-region method has been slightly increased due to the extra computations required to form the analytical Hessian. The number of iterations required for the Newton Trust-region optimization method using finite difference approximations of the Hessian has increase about 50% as compared with the iterations required for the Trust-region method using analytic Hessian expressions. Furthermore, the computational time for the Trust-region optimization method using finite difference approximations of the Hessian has increased by one order of magnitude. Finally, it should be noted that without providing the analytic expressions for the gradients of the objective function the algorithms present convergence problems for all cases.

Optimization method	3 parameters model		5 parameters model		7 parameters model	
	time (min)	Iterations	time (min)	Iterations	time (min)	Iterations
BFGS	0.62	14	0.85	21	0.95	26
Trust-region (approximate Hessian using finite difference)	4.16	50	4.02	31	7.88	47
Trust-region (analytic Hessian)	1.00	33	0.96	22	1.72	30

**Table 1: Comparison between computational time and number of iterations**

## 5 Conclusions

Model updating algorithms were proposed to characterize and compute all Pareto optimal models from a model class, consistent with the measured modal data and the norms used to measure the fit between the measured and model predicted modal properties. Computational algorithms for the efficient and reliable

solution of the resulting multi- and single-objective optimization problems were presented. The algorithms are classified to gradient-based, evolutionary strategies and hybrid techniques. The Normal Boundary Intersection method, in particular, is used as the gradient-based method to solve the multi-objective optimization. Efficient algorithms are introduced for reducing the computational cost involved in estimating the gradients of the objective functions. Specifically, a formulation requiring the solution of the adjoint eigen-problem is presented, avoiding the explicit estimation of the gradients of the eigenvalues and the eigenvectors. The adjoint method is also extended to carry out efficiently the estimation of the Hessian of the objective functions, avoiding the explicit estimation of the Hessian of the eigenvalues and eigenvectors. The computational cost for estimating the gradients is shown to be independent of the number of structural model parameters. The methodology is particularly efficient to system with several number of model parameters and large number of DOFs where repeated gradient evaluations are computationally quite time consuming. Gradient-based optimization algorithms such as the BFGS algorithm and the Newton Trust Region algorithm available in Matlab, exploit the proposed analytical gradients and Hessians estimates in order to significantly reduce the computational time. In particular, algorithms using finite difference approximations of the gradients or even Hessians are shown to perform poorly for modal-based finite element model updating applications. The effectiveness of the proposed optimization algorithms for finite element model updating by providing the analytic expression for the gradients and Hessian matrix of the objective functions was demonstrated using ambient measurements from a reinforced concrete bridge.

## Acknowledgements

This research was co-funded 75% from the European Union (European Social Fund), 25% from the Greek Ministry of Development (General Secretariat of Research and Technology) and from the private sector, in the context of measure 8.3 of the Operational Program Competitiveness (3<sup>rd</sup> Community Support Framework Program) under grant 03-EA-524 (PENED 2003). This support is gratefully acknowledged.

## References

- [1] J.E. Mottershead, M.I. Friswell, *Model updating in structural dynamics: A survey*, Journal of Sound and Vibration, Vol. 167 (1993), pp. 347-375.
- [2] C. Papadimitriou, J.L. Beck, L.S. Katafygiotis, *Updating robust reliability using structural test data*, Probabilistic Engineering Mechanics, Vol. 16 (2001), pp. 103-113.
- [3] C.P. Fritzen, D. Jennewein, T. Kiefer, *Damage detection based on model updating methods*, Mechanical Systems and Signal Processing, Vol. 12, No. 1 (1998), pp. 163-186.
- [4] A. Teughels, G. De Roeck, *Damage detection and parameter identification by finite element model updating*, Archives of Computational Methods in Engineering, Vol. 12, No. 2 (2005), pp. 123-164.
- [5] M.W. Vanik, J.L. Beck, S.K. Au, *Bayesian probabilistic approach to structural health monitoring*, Journal of Engineering Mechanics (ASCE), Vol. 126 (2000), pp. 738-745.
- [6] E. Ntotsios, C. Papadimitriou, P. Panetsos, G. Karaiskos, K. Perros, Ph. Perdikaris, *Bridge health monitoring system based on vibration measurements*, Bulletin of Earthquake Engineering (2008), in press
- [7] K.V. Yuen, J.L. Beck, *Reliability-based robust control for uncertain dynamical systems using feedback of incomplete noisy response measurements*, Earthquake Engineering and Structural Dynamics, Vol. 32, No. 5 (2003), pp. 751-770.
- [8] J.L. Beck, L.S. Katafygiotis, *Updating models and their uncertainties- I: Bayesian statistical framework*, Journal of Engineering Mechanics (ASCE), Vol. 124, No. 4 (1998), pp. 455-461.

- [9] R.B. Nelson, *Simplified calculation of eigenvector derivatives*, AIAA Journal, Vol. 14, No. 9 (1976), pp. 1201-1205.
- [10] Y. Haralampidis, C. Papadimitriou, M. Pavlidou, *Multi-objective framework for structural model identification*, Earthquake Engineering and Structural Dynamics, Vol. 34, No. 6 (2005), pp. 665-685.
- [11] K. Christodoulou, C. Papadimitriou, *Structural Identification Based on Optimally Weighted Modal Residuals*, Mechanical Systems and Signal Processing, Vol. 21 (2007), pp. 4-23.
- [12] L.S. Katafygiotis, *Treatment of Model Uncertainties in Structural Dynamics*, Technical Report EERL91-01, California Institute of Technology, Pasadena, CA. (1991).
- [13] L.S. Katafygiotis, J.L. Beck, *Updating models and their uncertainties. II: Model identifiability*, Journal of Engineering Mechanics (ASCE), Vol. 124, No. 4 (1998), pp. 463-467.
- [14] L.S. Katafygiotis, C. Papadimitriou, H.F. Lam, *A probabilistic approach to structural model updating*, International Journal of Soil Dynamics and Earthquake Engineering, Vol. 17 (1998), pp. 495-507.
- [15] L.S. Katafygiotis, H.F. Lam, *Tangential-projection algorithm for manifold representation in unidentifiable model updating models*, Earthquake Engineering and Structural Dynamics, Vol. 31, No. 4 (2002), pp. 791-812.
- [16] K. Christodoulou, E. Ntotsios, C. Papadimitriou, P. Panetstos., *Structural model updating and prediction variability using Pareto optimal models*, Comput. Methods Appl. Mech. Engrg. (2008), doi:10.1016/j.cma.2008.04.010
- [17] A. Teughels, G. De Roeck, J.A.K. Suykens, *Global optimization by coupled local minimizers and its application to FE model updating*, Computers and Structures, Vol. 81, No. 24-25 (2003), pp. 2337-2351.
- [18] H. G. Beyer, *The theory of evolution strategies*, Berlin, Springer-Verlag (2001).
- [19] E. Zitzler, L. Thiele, *Multi-objective evolutionary algorithms: A comparative case study and the strength Pareto approach*, IEEE Transactions on Evolutionary Computation, Vol. 3 (1999), pp. 257-271.
- [20] I. Das, J.E., Jr., Dennis, *Normal-Boundary Intersection: A new method for generating the Pareto surface in nonlinear multi-criteria optimization problems*, SIAM Journal of Optimization, Vol. 8 (1998), pp. 631-657.
- [21] E. Ntotsios, Ch. Karakostas, V. Lekidis, P. Panetsos, G. Nikolaou, C. Papadimitriou, *Structural Identification of Egnatia Odos Bridges based on Ambient and Earthquake Induced Vibrations*, Bulletin of Earthquake Engineering (2008), in press.
- [22] COMSOL AB (2005) *COMSOL Multiphysics User's Guide*. [<http://www.comsol.com/>].
- [23] T.F. Coleman, Y. Li, *An Interior, Trust Region Approach for Nonlinear Minimization Subject to Bounds*, SIAM Journal on Optimization, Vol. 6 (1996), pp. 418-445.
- [24] T.F. Coleman, Y. Li, *On the Convergence of Reflective Newton Methods for Large-Scale Nonlinear Minimization Subject to Bounds*, Mathematical Programming, Vol. 67, Number 2 (1994), pp. 189-224.
- [25] C.G. Broyden, *The Convergence of a Class of Double-Rank Minimization Algorithms*, Journal Inst. Math. Applic. (1970), Vol. 6, pp. 76-90.
- [26] R. Fletcher, *A New Approach to Variable Metric Algorithms*, Computer Journal (1970), Vol. 13, pp. 317-322.
- [27] D. Goldfarb, *A Family of Variable Metric Updates Derived by Variational Means*, Mathematics of Computing (1970), Vol. 24, pp. 23-26.
- [28] D.F. Shanno, *Conditioning of Quasi-Newton Methods for Function Minimization*, Mathematics of Computing (1970), Vol. 24, pp. 647-656.